Performance Comparison Analysis of a High Voltage DC LLC Resonant Converter for Telecom and Datacenter Applications

Ramesh B. Darla and **A. Chitra**†, Non-members

ABSTRACT

Intermediate Bus Architecture (IBA) is used for power distribution in information communication technology (ICT) equipment due to the flexibility of its power distribution and cost-effectiveness compared to centralized or DC-mediated power. The reason for IBA's good performance in this context is its greater reliability and efficient Intermediate Bus Converter (IBC). Existing IBAs comprise low-voltage systems with multiple power, resulting in power loss. This study outlines the need for a high-voltage DC-to-DC converter to solve the problems associated with conventional 48 VDC converters. A 300 W LLC series resonant converter is utilized for the design and analysis of converter efficiency and losses across various input voltages. The results indicate that the maximum converter efficiency is >92% at full load. MATHCAD is used to analyze the performance of the LLC converter and understand the suitable operating zones for zero-voltage-switching. The LLC converter's efficiency is investigated for multiple input voltage ranges. The LLC converter is designed and developed in MATLAB and the results of the simulation are presented. Trade-offs in the LLC converter's design are also discussed, with the goal of operating the converter in an optimal manner and achieving the maximum possible efficiency.

Keywords: LLC Resonant Converter, Telecom Power, MATHCAD Analysis, DC/DC Converters, MATLAB

1. INTRODUCTION

Over the last two decades, the ICT equipment power distribution systems used in networking applications have changed dramatically, primarily due to increasing performance requirements and cost-related factors. The major transition occurred in the 1990s when the industry introduced Distributed Power Architecture (DPA) as an alternative to centralized power supply [1–3]. The centralized power supply configuration is modified with the addition of a front-end power supply that converts AC into DC power and feeds the backplane of the rack, as presented in Fig. 1. Typically, the output voltage of a front-end power supply is 48 VDC. The ICT equipment installed in the backplane includes 48 VDC input DC-to-DC converter modules that supply all necessary voltages to ICT process loads, as shown in Fig. 1.

DPA-based power systems are capable of solving the conduction loss issues caused by load currents. They tend to afford additional flexibility to systems and slightly shorter design cycles, but the system costs remain relatively high. As line card supply voltages (ICT equipment) increase to four/five times the initial requirements [2], the question has arisen as to how many isolated converters per line card should be used [2, 4]. Narveson [4] suggested the use of a single discrete DC-to-DC converter of between 48 VDC and other load voltages. For instance, if the converter features a 12 VDC output, a point-of-load (POL) converter is used to derive the other load voltages from the 12 VDC one. The use of a single, isolated DC-to-DC converter and POL converter is the first step to introducing Intermediate Bus Architecture (IBA). The advantage of IBA is that the POL used to supply low voltages and high currents can be placed near the load. Placing the POL near the load decreases parasites in the power supply plane and improves the dynamic response of the current profile. Another advantage of IBA is the potential reduction in the cost of power distribution [2].

In addition, the demand from the analog and digital IC industries for different supply voltages, ranging from 0.8 VDC to 5 VDC and 12 VDC, and the availability of low-cost POLs, seeks to force the introduction of IBA [5–8]. The front-end AC-to-DC or DC-to-DC power supply is used to convert the input voltage to 48 VDC in IBA power distribution. An Intermediate Bus Converter (IBC) is used to nominally convert 48 VDC to 12 VDC, and this converter is an isolated DC-to-DC unit, and the 12 VDC bus termed an Intermediate Bus [2]. The POL converters are connected between intermediate buses and loads to provide voltage for the different analog and digital circuits, as shown in Fig. 2.

The DC-to-DC converter (IBC) is used with the intermediate bus to produce the intermediate bus voltage needed to achieve higher efficiency and better reliability at a lower cost. The first IBC converters in the industry were marginally updated variants of fully regulated DC-to-DC power converter modules [9]. IBCs rapidly

Manuscript received on April 15, 2022; revised on August 12, 2022; accepted on September 15, 2022. This paper was recommended by Associate Editor Kaan Kerdchuen.

The authors are with the School of Electrical Engineering, Vellore Institute of Technology, Vellore, India.

†Corresponding author: chitra.a@vit.ac.in

Digital Object Identifier: 10.37936/ecti-eec.2023211.248666

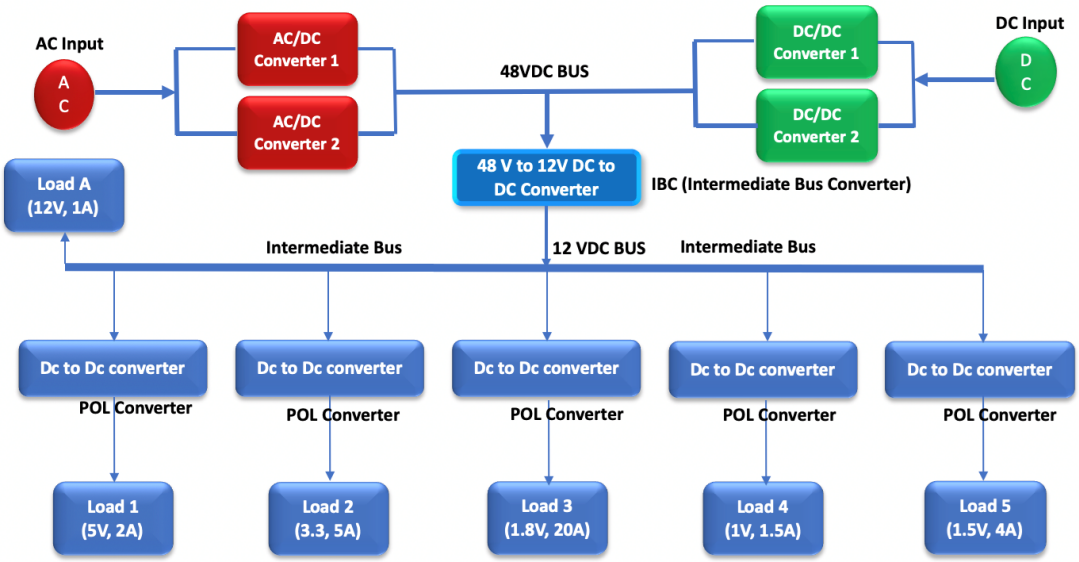

Fig. 1: Distributed power architecture.

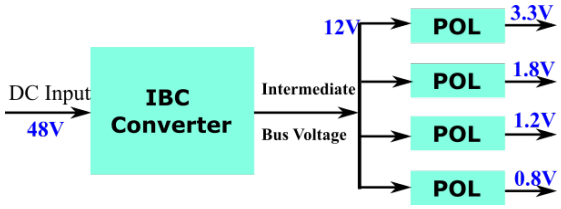

Fig. 2: Block diagram of intermediate bus architecture.

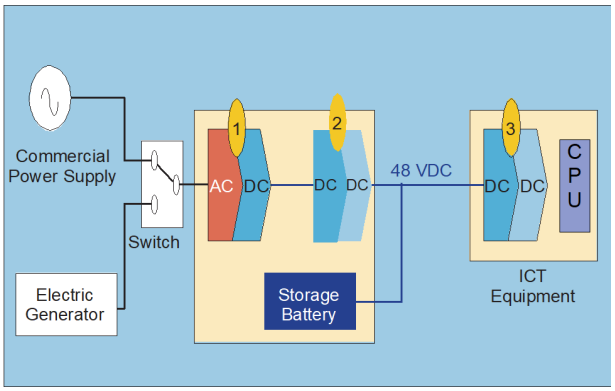

Fig. 3: Power conversion stages of existing intermediate bus architecture.

evolved into an independent specialty product within the portfolio of module manufacturing, due to their power density, efficiency, and cost requirements. Most IBCs have been standardized to operate from 48 VDC inputs and regulate 12 VDC output voltages with varying power levels at an efficiency of over 90% [9].

Current 48 VDC IBAs, which provide power from front-end power converters to IBCs, have the disadvantage of higher input voltage conversions to lower 48 V with the help of DC-to-DC converters within front-end power converter devices. There are four power conversion stages, from a front-end converter to the load point (Stage 4), as shown in Fig. 3, while the total system efficiency is lower due to greater power loss. System efficiency may be improved by eliminating the power conversion stages and reducing power loss. This indicates that the conversion stages 2 and 3, displayed in Fig. 3, can be eliminated by replacing one DC-to-DC converter.

The replacement converter uses a high-voltage DC input to deliver a low-voltage DC output. The input voltage ranges from 200–400 VDC [10–16] and the output voltage is 12 VDC. Research is underway to determine the optimal DC input voltage to achieve high efficiency and reliability at a low cost.

A resonant LLC converter is used for the IBC since it has the advantage of operating at higher frequencies with smaller footprints while attaining the requisite efficiency [17] and reliability [18, 19]. Another advantage of an LLC converter is that it has a higher power density with fewer components [3, 17, 18]. This study evaluates the LLC converter designed to obtain optimal DC voltage levels by considering efficiency and semiconductor switching losses [18].

The remainder of the paper is laid out as follows. Details of the LLC resonant converter circuit are specified in Section 2 with the DC characteristics of the converter outlined in Section 3. Section 4 shows a comparison of LLC power topologies. Section 5 presents the design methodology of the proposed LLC converter for the different input voltages. Section 6 describes the simulation model and results of the high-voltage input LLC resonant converters. Finally, the conclusion is presented in Section 7.

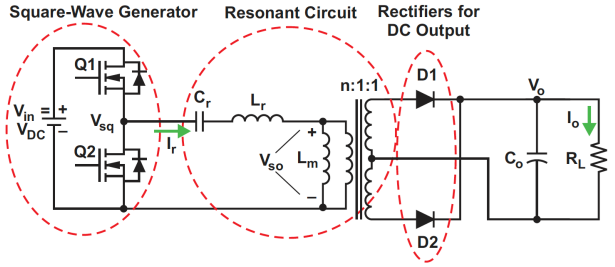

Fig. 4: LLC resonant half-bridge converter [25].

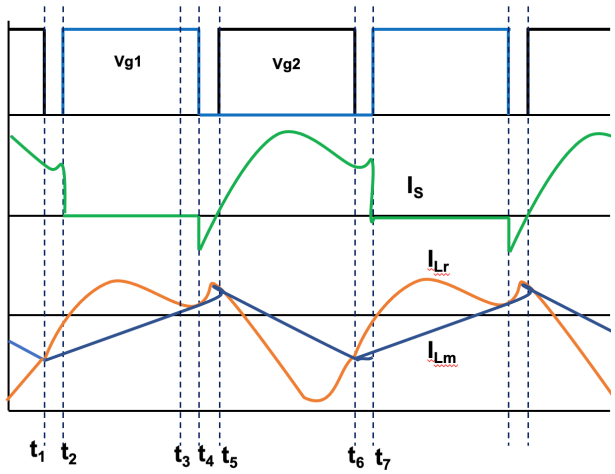

Fig. 5: Operational circuit waveforms of the LLC converter [25].

2. LLC SERIES RESONANT CONVERTER

Fig. 4 shows the basic circuit diagram of the LLC converter [19, 20], consisting of a primary side half-bridge switching circuit (square wave generator), an LC tank circuit, and a center-tap transformer followed by a half-bridge rectifier. The converter works with variable switching frequency control, with primary switches operating in a complementary fashion with a 180° phase shift with proper dead-time control. The operating waveforms shown in Fig. 5 concern the switching pulses of the Q_1 and Q_2 switches [20, 21].

As can be observed from Fig. 4, the circuit features a few passive components, such as C_r, L_r, and L_m, where L_r and C_r are the LLC series resonant inductor and capacitor, respectively, and L_m is the magnetizing inductor [19, 21]. The magnetizing inductance behaves as a shunt inductor [22].

Fig. 5 also displays the circuit switching waveforms. The frequency of operation is assumed to be the same as the resonance frequency calculated using the L_r and C_r. Due to the L_m, there is a considerable amount of magnetizing current (I_m) on the primary side that freewheels with it and plays no role in the transfer of power. The circuit current (I_p) is the sum of I_m and I_o referred to as the primary [22].

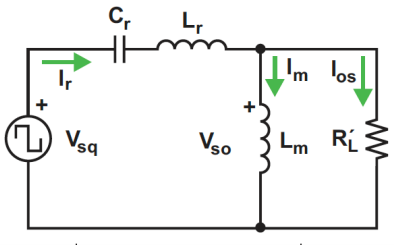

Fig. 6: LLC series resonant converter equivalent circuit.

The current flow is sinusoidal due to the capacitor and inductors in the tank circuit having a square wave voltage input. The tank circuit helps filter the high harmonic currents. Due to the inductance, the primary current lags behind the applied voltage, helping to achieve zero-voltage switching [21] of the metal-oxide-semiconductor field-effect transistor (MOSFET) [24]. The MOSFET is switched on when there is a current flow in its anti-parallel diode since the voltage over it is zero at this point. All the critical waveforms of the LLC converter are shown in Fig. 5, where one switching device current (I_s), series inductor current (I_{L_r}), and magnetizing current (I_{L_m}) are shown with respect to the gate pulse of the MOSFET.

The secondary rectifier circuit converts the alternating voltage from the LLC transformer into DC, which is then fed to the load. Detailed analyses of LLC converters can be found in the literature, e.g. [2, 22–25]. The secondary rectifier circuit can be a full-bridge type or half-bridge center tap. Synchronous rectification is widely used to enhance the power supply performance of more critical high-power applications, rather than diode rectifiers.

3. ANALYSIS OF THE LLC SERIES RESONANT CONVERTER

The function of any converter is to provide a specified output voltage at a given input voltage and applied load, with the output voltage remaining constant under changes in the input voltage and load. The converter must also fulfill the condition of achieving maximum efficiency by reducing loss. Therefore, for the LLC resonant converter to attain good output regulation, it is important to consider its DC characteristics, as discussed in this section. The equivalent circuit of the LLC derived from the first harmonic approximation (FHA) [18, 22, 23, 26, 27] is used to investigate and analyze the LLC converter's characteristics in the frequency domain. Fig. 6 displays the equivalent circuit of the LLC series resonant converter [28].

To simplify the equations in Fig. 6, the relationship between V_o and V_{in} can also be illustrated using the electrical circuit variables L_r, L_m, C_r, and R_{ac}. Therefore, the input to the output voltage gain or voltage transfer functions becomes:

$$M = \frac{V_o}{V_{in}} = \left| \frac{jX_{L_m} \parallel R_{ac}}{\left(jX_{L_m} \parallel R_{ac}\right) + j\left(X_{L_r} - X_{C_r}\right)} \right| = \left| \frac{j\omega L_m \parallel R_{ac}}{\left(j\omega L_m \parallel R_{ac}\right) + j\omega L_r + \frac{1}{j\omega C_r}} \right| \quad (1)$$

where $j = \sqrt{-1}$.

Eq. (1) depicts that a connection from the input voltage (V_{in}) to the output voltage (V_o) can be established in relation to M, with LLC circuit parameters such as:

- Resonant frequency

$$F_{r1} = \frac{1}{2\pi\sqrt{L_r C_r}} \quad (2)$$

- Normalised switching frequency

$$x1 = \frac{F_{sw}}{F_{r1}} \quad (3)$$

- Ratio of magnetizing inductance to resonating inductance

$$k = \frac{L_m}{L_r} \quad (4)$$

- Reflected load resistance

$$R_{ac} = \frac{8n^2 R_L}{\pi^2} \quad (5)$$

- Turns ratio

$$n = \frac{N_P}{N_S} \quad (6)$$

- Quality factor [19]

$$Q = \frac{\text{Energy stored}}{\text{Energy dissipated}} = \frac{2\pi F_{r1} L_r}{R_{ac}} = \frac{1}{2\pi F_{r1} C_r R_{ac}} = \frac{\sqrt{L_r/C_r}}{R_{ac}} \quad (7)$$

With the help of Eqs. (2)–(7), the voltage gain function can then be normalized and expressed as [28]

$$M = \frac{1}{\sqrt{\left[1 + \frac{1}{k^2} \times \left(1 - \frac{1}{x1^2}\right)\right]^2 + \left[Q \times \left(x1 - \frac{1}{x1}\right)\right]^2}} \quad (8)$$

$$V_o = M \times \frac{1}{n} \times \frac{V_{in}}{2} \quad (9)$$

$$\frac{V_o}{V_{in}} = \frac{M}{2n} \quad (10)$$

It can be observed from Eq. (10), the output voltage is calculated if the gain (M), transformer turns (n), and input voltage (V_{in}) are known.

The relationship between the input and output voltages obtained from Eqs. (8) and (9) can be written as follows:

$$V_o = M \times \frac{1}{n} \times \frac{V_{in}}{2} = M(x1, k, Q) \times \frac{1}{n} \times \frac{V_{DC}}{2} \quad (11)$$

Fig. 7 indicates various possible relationships among LLC converter characteristics. Each plot is defined with a constant value of k (k = 1, 5, 10, and 20) with respect to different Q values, ranging from 0.1–10. Several observations can be made based on the plots; consider Fig. 8 which is redrawn using the details from Fig. 7(b). Fig. 8 shows that lower Q value curves represent lighter load conditions, whereas higher Q curves represent higher load conditions. All Q curves are then shown to cross at one resonance frequency point ($x1$ = 1 or F_{sw} = F_{r1}) and exhibit a unity gain [24].

It is apparent that the peaks of the gain curve shown in Fig. 8 define the boundary conditions in the tank circuit between the two inductive and capacitive impedances. The shaded area on the left-hand side is the capacitive operating region and the inductive operating region of the LLC converter on the right. The purpose of defining the operating regions is to ensure they always perform in the inductive region of the entire input voltage, as well as the load range [24]. The converter's operation should be within the inductive region to perform zero-voltage switching (ZVS). The switch Q_1 (MOSFET) current flow must be reversed before another switch Q_2 (MOSFET) is switched off. When the MOSFET switches off, the reverse current flows into the MOSFET body diode, resulting in hard commutation until another MOSFET in the bridge is switched on. At this point, reverse recovery losses and noise may exist, inducing high current spikes and leading to device failure. It should be noted that the operating point ($x1$, M) = (1, 1) is independent of the loading condition. This means that as long as the unity of the voltage gain (M) can be retained, the switching frequency is at the resonant frequency (F_{r1}), regardless of the load current.

In other words, the frequency variance is reduced to a minimum in a system where the operating point is at ($x1$, M) = (1, 1) or in its vicinity. At ($x1$, M) = (1, 1), the series resonant circuit impedance is zero, given that parasitic power losses are not present. Instead, the total input voltage is applied to the output load regardless of the load current variation. However, the impedance of the series resonant circuit is a non-zero distance away from ($x1$, M) = (1, 1), the voltage gain varies according to load impedance, and the operation is load-dependent.

An increase in Q shrinks the curve for a fixed k, resulting in a narrower frequency control range being predicted because Q is the quality factor of the LLC converter series tank circuit. However, although the entire gain curve may show a downward trend, the

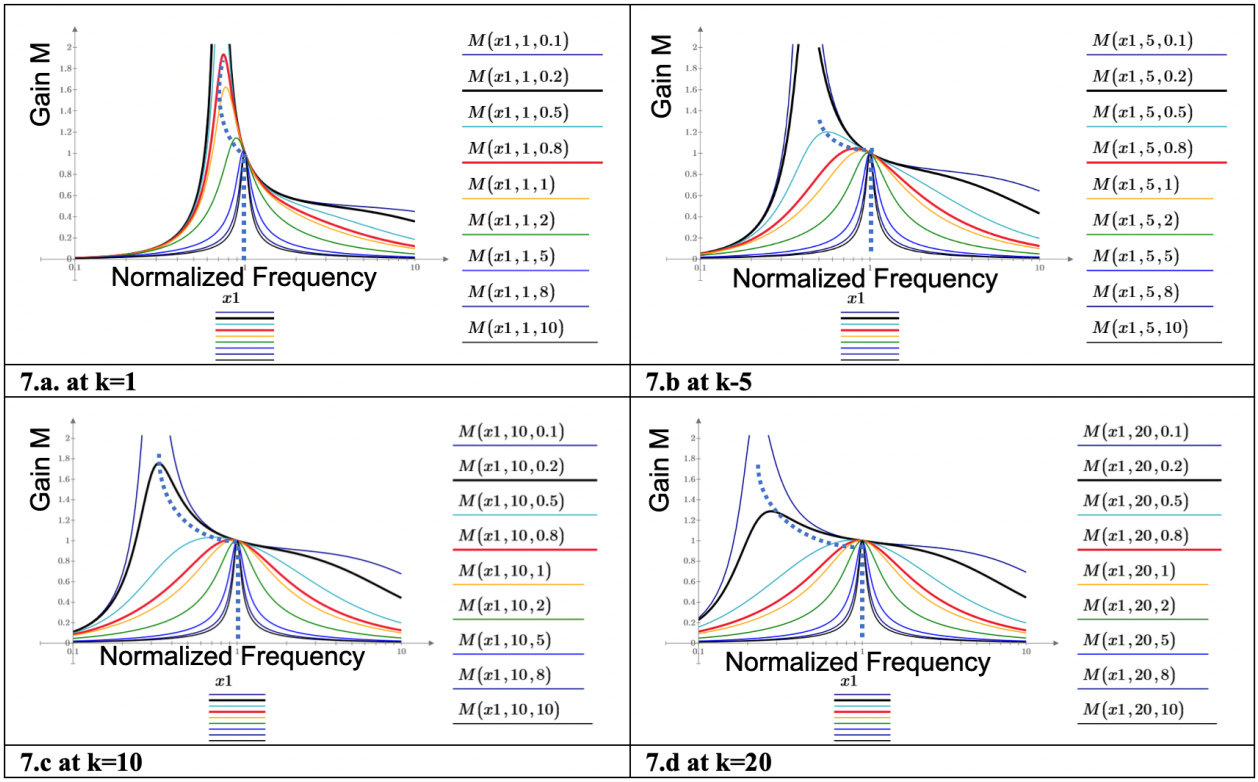

Fig. 7: *Voltage gain plots for different values of k ($k = L_m/L_r$).*

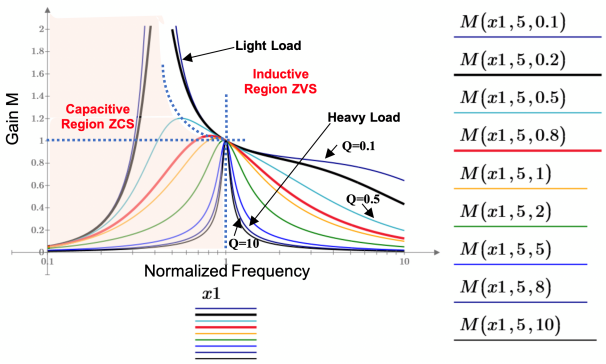

Fig. 8: *Gain curves with respect to boundary conditions ZVS-ZCS.*

respective gain M peak value is lower, as well as the $x1$, referring to a value that drops to the right and is nearer to $x1 = 1$. This frequency change is due to an increased load that rises with Q.

A review of Eqs. (5) and (7) implies that an increase in the Q value may lead to a decrease in load resistance (R_L) because L_m and L_r are fixed values. C_r is fixed to the same sequence of resonant frequencies, and R_L is parallel to L_m, so R_L would reduce the impact of L_m and move F_{r2} to F_{r1}. Therefore, if the R_L varies from no load (open) to full load (short), the peak resonant gain values decrease from infinity to one, while the relative peak resonance frequency also shifts from F_{r2} to the resonant frequency series (F_{r1}).

Furthermore, the achievement of performance improvement is significant, with tight regulation for given input and output conditions, and therefore understanding the impact of ratio k (L_m/L_r) on the converter's operation. Fig. 9 displays the curves of the resonant tank gain for various values of k to demonstrate the latter's impact. Apart from the narrower frequency modulation range, it is evident that lower k values can deliver better boost gains, meaning that the converter will feature more robust regulation and control, making it suitable for projects with wide input voltage ranges [25].

4. COMPARISON OF LLC POWER TOPOLOGIES

To increase the efficiency and reliability of the converter, it is important to select the optimum power topology. Qualitative analysis is presented to choose the optimum LLC converter. There are certain factors to consider when choosing the topology since it must meet the power density, efficiency, and reliability requirements within the given form. A comparative study is helpful for choosing the best topology among those available in the literature. Table 1 presents a comparison of different power topologies.

From Table 1, it can be observed that topology 8 has more switches, magnetics, and resonant components, while topology 1 has fewer switches, magnetics, and resonant components. All the topologies can transfer the required power levels for a given input to output.

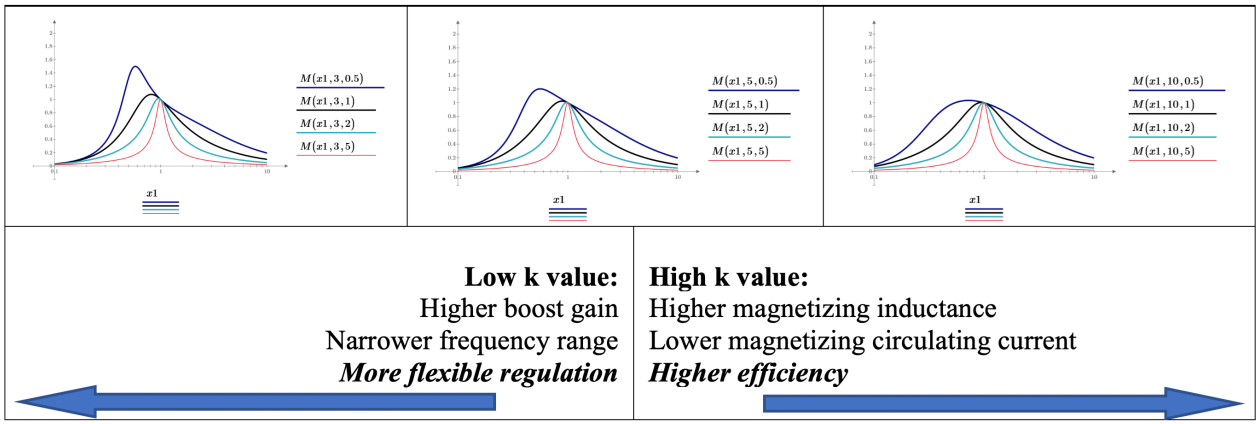

Fig. 9: Converter operation transition gains.

Table 1: Power topology comparison.

Type	Topology	Switches	Diodes	Transformers	Inductors	E-Cap	R-Cap
Non-interleaved	Topology 1 [29]	2	2	1	1	1	1
	Topology 2 [30]	4	2	1	1	1	1
	Topology 3 [31]	4	2	1	1	1	1
	Topology 4 [30, 31]	6	0	1	1	1	1
Interleaved	Topology 5 [32, 33]	8	0	2	2	1	2
	Topology 6 [34]	12	6	3	3	1	3
	Topology 7 [35]	6	4	2	2	1	2
	Topology 8 [36]	12	0	3	3	3	3

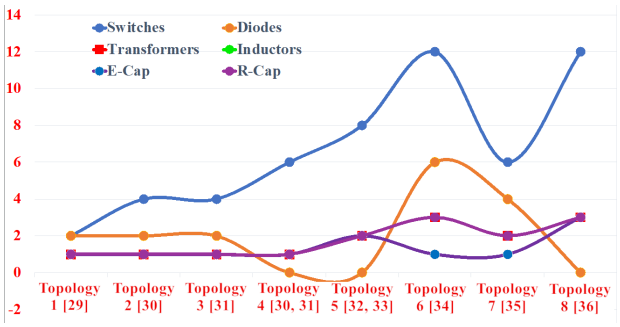

Fig. 10: Comparison of reviewed topologies.

Fig. 10 shows a comparison of the reviewed topologies. According to the results, topology 4 is the most efficient. Topology 1 (shown in Fig. 4) is chosen for this study since it has a smaller number of components and gives an acceptable efficiency range [29].

5. DESIGN OF THE LLC CONVERTER

The design example applies to the DC-to-DC converter for ICT loads requiring an output of 12 VDC at 25 A. The objective of this study is to design a converter that can operate with a DC input voltage of 270 to 450 VDC to provide 12 VDC at a full load current of 25 A.

Table 2: Technical specifications.

Parameter	Value
Input voltage (V_{in})	270–450 VDC
Output voltage (V_o)	12 VDC
Output load current (I_o)	25 A
Output load power (P_o)	300 W
Switching frequency	100 kHz

5.1 Design Steps

The design of the LLC can be undertaken by calculating the transformer turn ratio n and the minimum and maximum voltage gains of the resonant tank circuit. The equations provided in Section 3 are used to calculate the circuit parameters for the given converter specifications as shown in Table 2.

The proposed design assumes a nominal input voltage of 400 VDC, whereas the maximum frequency ($F_{\max}$) is 150 kHz and the minimum frequency ($F_{\min}$) is 100 kHz, respectively.

Using the equations in Section 3, the circuit parameters are calculated as follows:

Transformer turns ratio n = 16

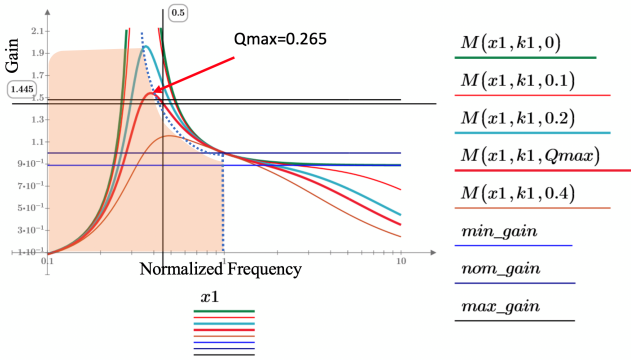

***Fig. 11**: Gain plot of DC-to-DC converter for the given specifications.*

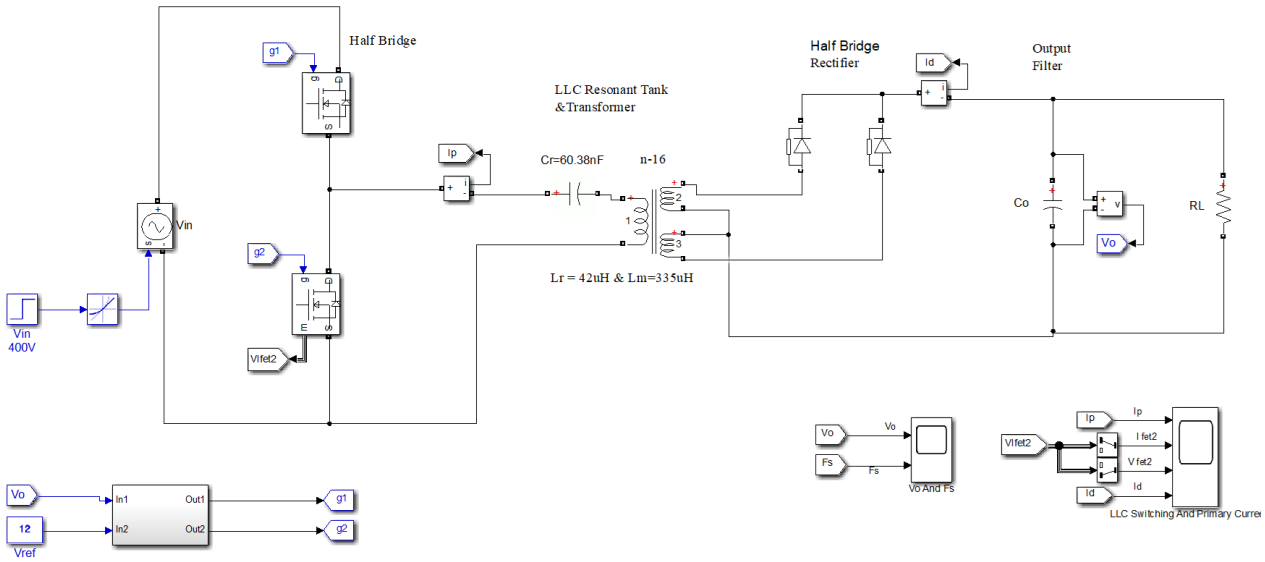

***Fig. 12**: MATLAB simulation model of the LLC series resonant converter.*

$$C_r = \frac{1}{2 * \pi * F_r * Z_r} = 60.38\ \mu\text{F}$$

$$L_r = \frac{Z_r}{2 * \pi * F_r * Z_r} = 41.95\ \mu\text{H}$$

$$L_m = L_r * k = 335\ \mu\text{H}$$

The above resonant frequency of 100 kHz corresponds to L_m = 335 μH and L_r = 41.95 μH, while the minimum frequency is determined as 45.89 kHz.

It is important to calculate the maximum Q value at the minimum input voltage since the power is detracted from the lower input voltage, as indicated in the specification. In the same manner, the maximum gain at the minimum switching frequency can be calculated using the maximum Q value. The same observations are apparent in the gain plot presented in Fig. 11.

The above plot displays the variation in the voltage gain with respect to the frequency. The red curve corresponds to full-load conditions (Q = Q_{max} = 0.265). To design the LLC tank components for optimized operation over a voltage variation of 270–450 V, it is necessary to ensure the no-load (Q = 0, green) and full-load (Q = Q_{max}, red) curves intersect with the minimum gain (min_gain = 0.889), nominal gain (nom_gain = 1.0) and maximum gain (max_gain = 1.481) shown on the vertical axis, and within the frequency boundaries.

6. CIRCUIT SIMULATION AND TEST RESULTS

All LLC converter parameters tabulated are calculated and outlined in Section 3.

6.1 MATLAB Simulation Diagram

The functional operation of the LLC converter is verified by the MATLAB model shown in Fig. 12, while all the circuit parameters are presented in Table 3. The operation is verified at one input voltage of 400 VDC from the light load to the full one. Based on the operation, it can be observed that the frequency varies with respect to load changes when the input remains constant, while the change frequency is within the maximum and minimum limits.

Figs. 13 to 15 show the converter switching behavior at different loading and input voltages. Fig. 13(a) displays

***Table 3**: LLC resonant converter circuit design parameters.*

Parameter	Value
Resonant frequency (F_{r1})	106 kHz
Minimum switching frequency	45.9 kHz
Resonant capacitor (C_r)	60.38 nF
LLC transformer specifications	
Turns ratio N_p:N_s	16
Leakage (resonant) inductor (L_r)	41.95 μH
Magnetizing inductor (L_m)	335 μH

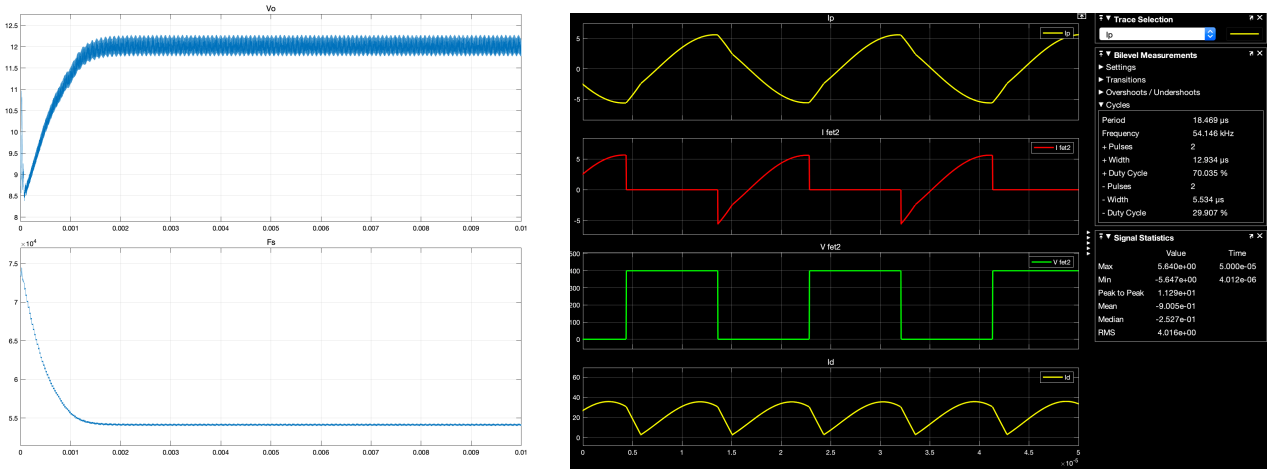

(a) *(b)*

***Fig. 13**: Test conditions: 300 W load with 400 VDC input voltage: (a) output voltage and switching frequency and (b) I_p, MOSFET current and voltage, and secondary diode current.*

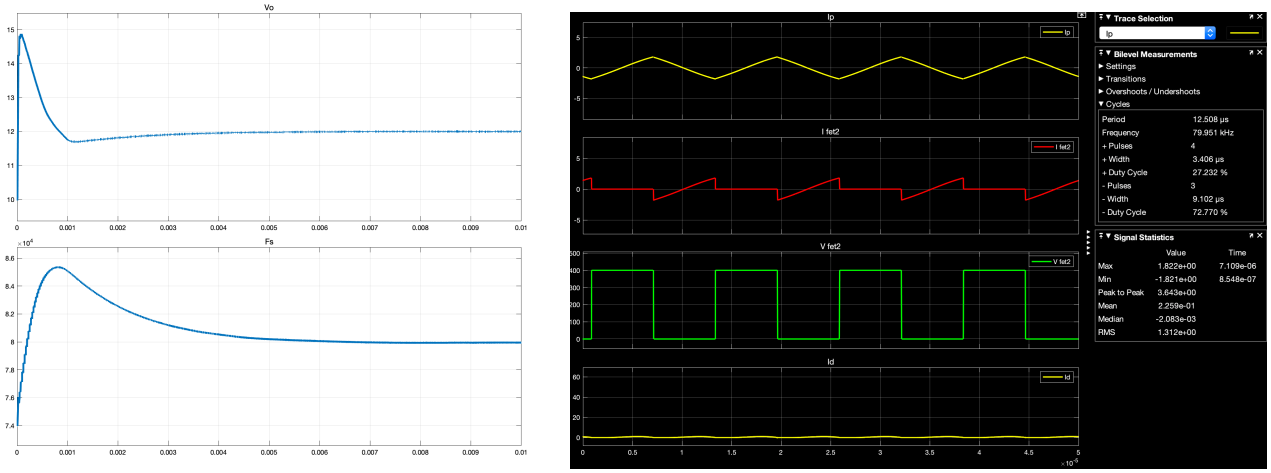

(a) *(b)*

***Fig. 14**: Test conditions: 6 W load with 400 VDC input voltage: (a) output voltage and switching frequency and (b) I_p, MOSFET current and voltage, and secondary diode current.*

the measured output voltage V_o and switching frequency F_{sw} under full-load (300 W) condition. Fig. 13(b) shows the primary current, secondary diode current, V_{DS}, and I_{DS} of the Q_2 power switch under full-load condition, during which ZVS is achieved.

Fig. 14(a) shows the measured output voltage V_o and the F_{sw} under light load (6 W) condition. Fig. 14(b) shows the primary current, secondary diode current, V_{DS}, and I_{DS} of the power switch Q_2 under light load condition, when ZVS is attained.

Similarly, Fig. 15(a) shows the measured output voltage V_o and the F_{sw} under 2 W load condition. Fig. 15(b) shows the primary current, secondary diode current, V_{DS}, and I_{DS} of the power switch Q_2 under 2 W load

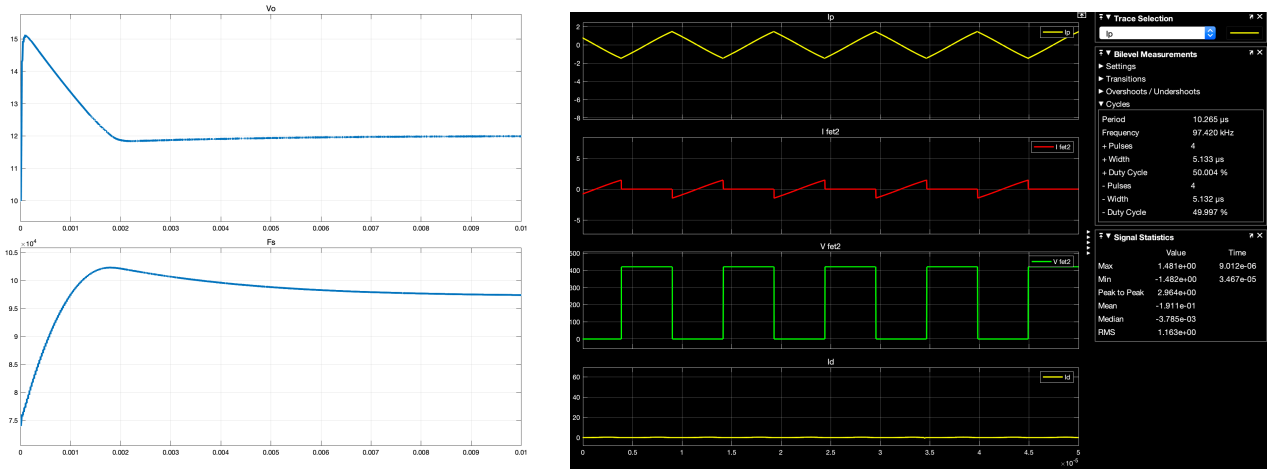

(a) (b)

***Fig. 15**: Test conditions: 6 W load with 400 VDC input voltage: (a) output voltage and switching frequency and (b) I_p, MOSFET current and voltage, and secondary diode current.*

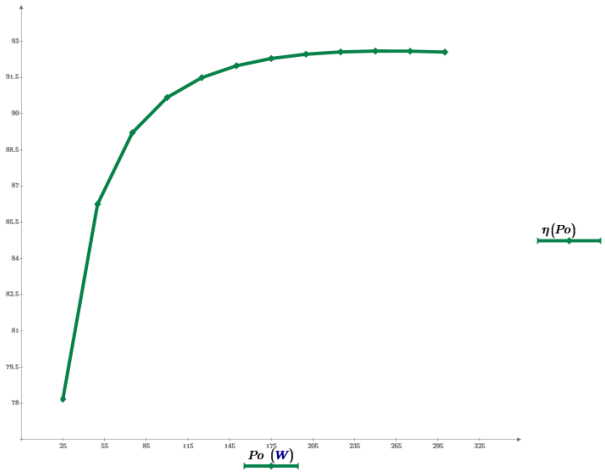

***Fig. 16**: Calculated efficiency of the converters; no load to full load at 400 V input.*

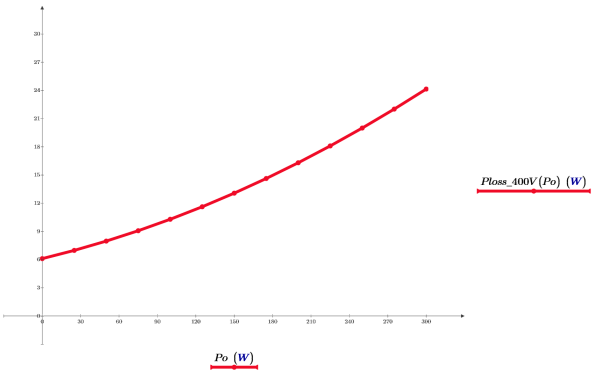

***Fig. 17**: Calculated converter power losses from no load to full load at 400 V input.*

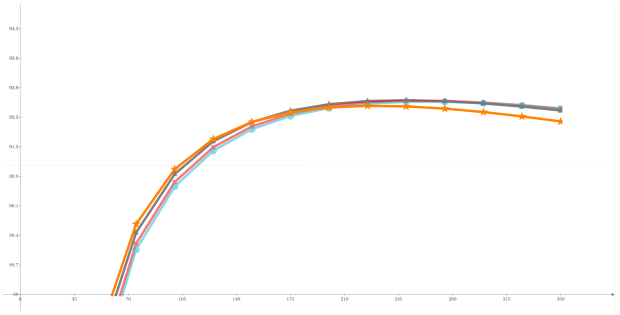

***Fig. 18**: Efficiency of the converter from no load to full load at different input voltages.*

conditions, when ZVS is attained.

The calculated efficiency of the converter is shown in Fig. 16. As can be observed, the efficiency is >92% in the LLC resonant converter under full-load conditions. Fig. 17 displays the variation in the losses of the LLC converter from no load to full load, when the input voltage is 400 V.

Fig. 18 shows the efficiency of the LLC converter with respect to different input voltages. The 200 V curve exhibits greater efficiency until 60% of the load is reached but then starts to deteriorate. The efficiency curve of the 400 V and 450 V is shown to be less efficient under light conditions and better with a 50 to 100% load. Accordingly, it can be concluded that the converter with a higher voltage input is also more efficient.

7. CONCLUSION

This study discusses the evolution of DPA, as well as the IBA for ICT equipment used for telecom and networks. The issues associated with the IBA and IBC converters are discussed to demonstrate the need for high-voltage DC-to-DC converters. An analysis of the LLC converter's DC characteristics is presented with the

aid of MATHCAD. The efficiency of the LLC converter for different input voltages is also discussed and compared. As can be observed, the power losses within the converter are higher at lower input voltages and lower at higher input voltages. Moreover, as demonstrated by the simulated test results, the rectifier diode losses in the LLC's resonant converter represent a large portion of the total power loss. The findings reveal that high-voltage input converters can address these issues and challenges by implementing IBC in a DPA configuration. By following the appropriate design methods, conventional IBCs can easily be replaced by high-voltage DC-to-DC converters. The simulation results of the 300 W output and 400 VDC input half-bridge DC-to-DC converters confirm the viability of the proposed improvements in the circuit.

REFERENCES

[1] P. Lindman and L. Thorsell, "Applying distributed power modules in telecom systems," *IEEE Transactions on Power Electronics*, vol. 11, no. 2, pp. 365–373, Mar. 1996.

[2] R. Miftakhutdinov, L. Sheng, J. Liang, J. Wiggenhorn, and H. Huang, "Advanced control circuit for intermediate bus converter," in *2008 Twenty-Third Annual IEEE Applied Power Electronics Conference and Exposition*, Austin, TX, USA, 2008, pp. 1515–1521.

[3] B. Yang, F. Lee, A. Zhang, and G. Huang, "LLC resonant converter for front end DC/DC conversion," in *Seventeenth Annual IEEE Applied Power Electronics Conference and Exposition*, vol. 2, Dallas, TX, USA, 2002, pp. 1108–1112.

[4] B. Narveson, "How many isolated DC-DC's do you really need?" in *Proceedings of Applied Power Electronics Conference. APEC '96*, vol. 2, San Jose, CA, USA, 1996, pp. 692–695.

[5] D. G. Morrison, "Distributed power moves to intermediate voltage bus," *Electronic Design*, pp. 55–62, Sep. 16, 2002.

[6] R. White, "Emerging on-board power architectures," in *Eighteenth Annual IEEE Applied Power Electronics Conference and Exposition. APEC '03*, vol. 2, Miami Beach, FL, USA, 2003, pp. 799–804.

[7] F. M. Miles, "An alternative power architecture for next generation systems," in *The 4th International Power Electronics and Motion Control Conference. IPEMC 2004*, vol. 1, Xi'an, China, 2004, pp. 67–72.

[8] M. Salato, "Datacenter power architecture: IBA versus FPA," in *2011 IEEE 33rd International Telecommunications Energy Conference (INTELEC)*, Amsterdam, Netherlands, 2011.

[9] M. Barry, "Design issues in regulated and unregulated intermediate bus converters," in *Nineteenth Annual IEEE Applied Power Electronics Conference and Exposition. APEC '04*, vol. 3, Anaheim, CA, USA, 2004, pp. 1389–1394.

[10] J. Zhu and S. Dou, "Intermediate bus voltage optimization for high voltage input VRM," in *2006 7th International Conference on Electronic Packaging Technology*, Shanghai, China, 2006.

[11] T. Yamashita, S. Muroyama, S. Furubo, and S. Ohtsu, "270 V DC system-a highly efficient and reliable power supply system for both telecom and datacom systems," in *21st International Telecommunications Energy Conference. INTELEC '99*, Copenhagen, Denmark, 1999.

[12] A. Matsumoto, A. Fukui, T. Takeda, and M. Yamasaki, "Development of 400-vdc output rectifier for 400-vdc power distribution system in telecom sites and data centers," in *IEEE 32nd International Telecommunications Energy Conference (INTELEC)*, Orlando, FL, USA, 2010.

[13] D. P. Symanski, "Why not operate data centers & telecom central offices at 400 vdc???" in *2009 IBM Power and Cooling Technology Symposium*, 2009.

[14] A. Pratt, P. Kumar, and T. V. Aldridge, "Evaluation of 400V DC distribution in telco and data centers to improve energy efficiency," in *INTELEC 07 - 29th International Telecommunications Energy Conference*, Rome, Italy, 2007, pp. 32–39.

[15] F. Bodi and E. H. Lim, "380/400V DC powering option," in *2011 IEEE 33rd International Telecommunications Energy Conference (INTELEC)*, Amsterdam, Netherlands, 2011.

[16] EMerge Alliance, "380 Vdc architectures for the modern data center," 2013.

[17] C. Fei, F. C. Lee, and Q. Li, "High-efficiency high-power-density LLC converter with an integrated planar matrix transformer for high-output current applications," *IEEE Transactions on Industrial Electronics*, vol. 64, no. 11, pp. 9072–9082, Nov. 2017.

[18] G. Ivensky, S. Bronshtein, and A. Abramovitz, "Approximate analysis of resonant LLC DC-DC converter," *IEEE Transactions on Power Electronics*, vol. 26, no. 11, pp. 3274–3284, Nov. 2011.

[19] R.-L. Lin and L.-H. Huang, "Efficiency improvement on LLC resonant converter using integrated LCLC resonant transformer," *IEEE Transactions on Industry Applications*, vol. 54, no. 2, pp. 1756–1764, Mar. 2018.

[20] J. Zeng, G. Zhang, S. S. Yu, B. Zhang, and Y. Zhang, "LLC resonant converter topologies and industrial applications — a review," *Chinese Journal of Electrical Engineering*, vol. 6, no. 3, pp. 73–84, Sep. 2020.

[21] H. Choi, "Analysis and design of LLC resonant converter with integrated transformer," in *APEC 07 - Twenty-Second Annual IEEE Applied Power Electronics Conference and Exposition*, Anaheim, CA, USA, 2007, pp. 1630–1635.

[22] T. Tanaka, N. Hanaoka, A. Takahashi, K. Asakimori, T. Iwato, A. Sakurai, and N. Yamashita, "Concept of new power supply system topology using 380 V and 48 V DC bus for future datacenters and telecommunication buildings," in *2015 IEEE International Telecommunications Energy Conference (INTELEC)*, Osaka, Japan, 2015.

[23] H.-S. Choi, "Half-Bridge LLC Resonant Converter Design Using FSFR-Series Fairchild Power Switch (FPS™)," onsemi, Aurora, Colorado, USA, No. AN-4151, 2014. [Online]. Available: https://www.onsemi.com/pub/Collateral/AN-4151.pdf

[24] C.-A. Cheng, H.-W. Chen, E.-C. Chang, C.-H. Yen, and K.-J. Lin, "Efficiency study for a 150W LLC resonant converter," in *2009 International Conference on Power Electronics and Drive Systems (PEDS)*, Taipei, Taiwan, 2009, pp. 1261–1265.

[25] H. Huang, "Designing an LLC resonant half-bridge power converter," Texas Instruments, Dallas, Texas, USA, No. SLUP263, 2010. [Online]. Available: https://www.ti.com/seclit/ml/slup263/slup263.pdf

[26] I.-O. Lee and G.-W. Moon, "The k-Q analysis for an LLC series resonant converter," *IEEE Transactions on Power Electronics*, vol. 29, no. 1, pp. 13–16, Jan. 2014.

[27] G. Pledl, M. Tauer, and D. Buecherl, "Theory of operation, design procedure and simulation of a bidirectional LLC resonant converter for vehicular applications," in *2010 IEEE Vehicle Power and Propulsion Conference*, Lille, France, 2010.

[28] A. K. Peter and J. Mathew, "A single phase, single stage AC-DC multilevel LLC resonant converter with power factor correction," *IEEE Access*, vol. 9, pp. 70 884–70 895, 2021.

[29] Y.-C. Lin, D.-T. Chen, and C.-J. Chen, "Flux-balance control for LLC resonant converters with center-tapped transformers," *Energies*, vol. 12, no. 17, 2019, Art. no. 3211.

[30] J.-W. Kim and G.-W. Moon, "A new LLC series resonant converter with a narrow switching frequency variation and reduced conduction losses," *IEEE Transactions on Power Electronics*, vol. 29, no. 8, pp. 4278–4287, Aug. 2014.

[31] Y. Shen, W. Zhao, Z. Chen, and C. Cai, "Full-bridge LLC resonant converter with series-parallel connected transformers for electric vehicle on-board charger," *IEEE Access*, vol. 6, pp. 13 490–13 500, 2018.

[32] Z. Hu, Y. Qiu, L. Wang, and Y.-F. Liu, "An interleaved LLC resonant converter operating at constant switching frequency," *IEEE Transactions on Power Electronics*, vol. 29, no. 6, pp. 2931–2943, Jun. 2014.

[33] K.-H. Yi and G.-W. Moon, "Novel two-phase interleaved LLC series-resonant converter using a phase of the resonant capacitor," *IEEE Transactions on Industrial Electronics*, vol. 56, no. 5, pp. 1815–1819, May 2009.

[34] H.-S. Kim, J.-W. Baek, M.-H. Ryu, J.-H. Kim, and J.-H. Jung, "The high-efficiency isolated AC–DC converter using the three-phase interleaved LLC resonant converter employing the Y-connected rectifier," *IEEE Transactions on Power Electronics*, vol. 29, no. 8, pp. 4017–4028, Aug. 2014.

[35] M. Salem, V. K. Ramachandaramurthy, A. Jusoh, S. Padmanaban, M. Kamarol, J. Teh, and D. Ishak, "Three-phase series resonant DC-DC boost converter with double LLC resonant tanks and variable frequency control," *IEEE Access*, vol. 8, pp. 22 386–22 399, 2020.

[36] H. Wang, Y. Chen, Y.-F. Liu, J. Afsharian, and Z. Yang, "A passive current sharing method with common inductor multiphase LLC resonant converter," *IEEE Transactions on Power Electronics*, vol. 32, no. 9, pp. 6994–7010, Sep. 2017.

Ramesh B. Darla received the B.Tech. Degree in electrical engineering from Akula Sree Ramulu College of Engineering, Jawaharlal Nehru Technological University, Hyderabad, India, an M.E. degree in electrical engineering from College of Engineering, Pune, India, and is currently pursuing a Ph.D. degree at School of Electrical Engineering, Vellore Institute of Technology, Vellore, India. He is currently working with Cisco Systems, Bengaluru, India. His fields of interest are power converters, PWM techniques, artificial neural networks, solar chargers, battery chargers, failure analysis, reliability aspects of power converters, component quality technologies and packaging.

A. Chitra received Bachelor of Engineering in Electrical and Electronics from Government College of Engineering, Tirunelveli, India. She completed her Master of Technology (Electric Drives and Control) in Pondicherry Engineering College, Puducherry, India. She received the Gold Medal from Pondicherry University for University First Rank in M.Tech (PED). She received her Ph.D. from Pondicherry University, India. She has been engaged in teaching and research work for the past 20 years in the area of Power Electronics, Renewable Energy Systems and Intelligent Drives. She is currently working as an Associate Professor in the School of Electrical Engineering, at Vellore Institute of Technology, Vellore, India. Her research areas include PV based systems, neural networks, induction motor drives, reliability analysis of multilevel inverters, and electrical vehicles.